Mechanics, Electronics, Automation and Automatic Control
T. Xia (Ed.)

doi:10.3233/SAEM240019

Analysis of an Interface Crack in Two-Dimensional Piezoelectric Materials Under Impact Loading

Lijie ZHANG and Ruifeng ZHANG[1]
Ningxia Institute of Science and Technology, Shizuishan, China
ORCiD ID: Ruifeng ZHANG https://orcid.org/0009-0008-0158-1130

Abstract. Based on the extended finite element method (XFEM), the problem of interface crack propagation in two-dimensional piezoelectric materials under impact loading is analyzed. By embedding the enrichment techniques as well as the partition of unity method (PUM) into the standard finite element approximation spaces, discontinuity problems can be fully processed. The major difference between the XFEM and the conventional finite element method (CFEM) is that the mesh in XFEM is independent of the internal geometry and physical interfaces, therefore there is no meshing and re-meshing difficulty in discontinuous problems. In this work, the stress and electrical displacement fields around a crack are analyzed. By using the interaction integral method, the fracture parameters, consisting of the stress intensity factors and the electrical displacement intensity factor, are evaluated. The influences of the geometric dimensions and external loads on the field intensity factors are discussed. In addition, the crack propagation problem is studied. The distribution of stress and electric field around the crack is given, and the influence of impact loading on the crack extension is emphatically discussed. To assess the accuracy of the proposed approach, the results obtained are compared with the analytical solutions, and consistent results were obtained.

Keywords. Extended finite element method, field intensity factor, piezoelectric materials, impact load, crack propagation

1. Introduction

The fracture and failure issues of piezoelectric materials have attracted widespread attention in the academic community since the publication of Parton's work [1-2] and significant achievements have been made in various aspects, including constitutive theory, numerical simulation, and experimental determination of piezoelectric materials [3-9]. The major research efforts have been summarized in several recently published review articles [10-11]. Due to the complexity of the issues, there are still many crucial problems to be further investigated in this research field. For instance, in order to simplify the derivation process, it is generally assumed that cracks are electrically impermeable, whereas cracks in practical engineering materials often contain air or vacuum inside. Although the dielectric coefficient is very small, the normal electric displacement component induced inside the crack cannot be completely neglected. Secondly, due to the difficulty in model simplification and mathematical solution for

[1] Corresponding Author: Ruifeng ZHANG, zrf_0353@163.com.

planar problems, the current research on the Type I crack of piezoelectric materials is relatively limited. In addition, most of the existing research focuses on single loading and static fracture issues. In fact, piezoelectric devices usually operate under complex loading environments of multi-field coupling or dynamic fields, such as mechanical, electrical, thermal, and magnetic fields. Therefore, further research is needed on dynamic fracture issues under complex loading conditions.

Most fracture problems in piezoelectric materials are analyzed with the aid of numerical methods. Boundary element method (BEM) is particularly suitable for crack problems but is not able to directly handle the geometrically identical crack surfaces. In addition, the finite element method (FEM) can be applied to solve crack problems in piezoelectric materials, but the remeshing in crack propagation simulation is a cumbersome task indeed. Furthermore, the boundary element-free method and many other methods have also been introduced. In recent years, the extended finite element method (XFEM) has been successfully developed and applied to solve many discontinuity problems in a wide range of engineering applications. The major difference between the XFEM and the conventional finite element method (CFEM) is that the mesh in XFEM is independent of the internal geometry and physical interfaces, thus overcoming meshing and re-meshing difficulties in discontinuous problems can be overcome.

In this work, based on the extended finite element method (XFEM), the problem of an interface crack in two-dimensional piezoelectric materials under impact loading is analyzed.

2. Basic theory

The basis of XFEM is partition of unity method (PUM). The basic idea of PUM is that any function $\Psi(x)$ can be expressed a set of local function $\mathrm{N}_I(x)\Phi(x)$ in domain:

$$\Psi(x) = \sum_I N_I(x)\Phi(x) \tag{1}$$

Here, meet the partition of unity $N_I(x) = 1, \Phi(x)$ is enriched functions.

XFEM extends the piecewise polynomial function space of conventional finite element methods with extra functions:

$$u^h(x) = \sum_{I \in N} N_I(x)[u_I + H(x)a_I + \sum_{\alpha=1}^{4} F_\alpha(x)b_I^\alpha] \tag{2}$$

where, u_I is the nodal DOF for conventional shape functions, $H(x)$ is heaviside distribution, a_I is nodal enriched DOF (jump discontinuity) , $F_\alpha(x)$ is crack tip asymptotic functions, b_I^α is the nodal DOF for crack tip enrichment .The crack is located using the level set method.

$$H(x) = \begin{Bmatrix} 1 & if\,(x - x^*)n \geq 0 \\ -1 & otherwise \end{Bmatrix} \tag{3}$$

Here x is an integration point, x* is the closest point to x on the crack face and n is the unit normal at x*.

The approximation of the displacement field in XFEM for interface crack takes the following form:

$$
\begin{aligned}
u^h(x) &= \sum_{i \in N^i} N_i(x) u_i [H(x) - H(x_j)] a_j \\
&+ \sum_{t \in N^{tip}} N_k(x) \sum_{\alpha=1}^{12} [F_\alpha(x) - F_\alpha(x_k)] b_{k\alpha} \\
&+ \sum_{I \in N^{interface}} N_I(x) \Psi(x) c_I
\end{aligned} \tag{4}
$$

It is important to note that $N^{interface}$ is the node set determined by the interface. The enrichment functions is takes the form of:

$$
\begin{aligned}
[F_\alpha(x), \alpha = 1,2...,12] = \Big\{ & \sqrt{r}\cos(\varepsilon \log r) e^{-\varepsilon\theta} \sin\frac{\theta}{2}, \quad \sqrt{r}\cos(\varepsilon \log r) e^{-\varepsilon\theta} \cos\frac{\theta}{2}, \\
& \sqrt{r}\cos(\varepsilon \log r) e^{\varepsilon\theta} \sin\frac{\theta}{2}, \quad \sqrt{r}\cos(\varepsilon \log r) e^{\varepsilon\theta} \cos\frac{\theta}{2}, \\
& \sqrt{r}\cos(\varepsilon \log r) e^{-\varepsilon\theta} \sin\frac{\theta}{2}\sin\theta, \sqrt{r}\cos(\varepsilon \log r) e^{\varepsilon\theta} \cos\frac{\theta}{2}\sin\theta, \\
& \sqrt{r}\sin(\varepsilon \log r) e^{-\varepsilon\theta} \sin\frac{\theta}{2}, \quad \sqrt{r}\sin(\varepsilon \log r) e^{-\varepsilon\theta} \cos\frac{\theta}{2}, \\
& \sqrt{r}\sin(\varepsilon \log r) e^{\varepsilon\theta} \sin\frac{\theta}{2}, \quad \sqrt{r}\sin(\varepsilon \log r) e^{\varepsilon\theta} \cos\frac{\theta}{2}, \\
& \sqrt{r}\sin(\varepsilon \log r) e^{\varepsilon\theta} \sin\frac{\theta}{2}\sin\theta, \sqrt{r}\cos(\varepsilon \log r) e^{\varepsilon\theta} \cos\frac{\theta}{2}\sin\theta \Big\}
\end{aligned} \tag{5}
$$

Similarly, the approximation of the electric potential field takes the following form:

$$
\begin{aligned}
\varphi^h(x) &= \sum_{i \in N^i} N_i(x) u_i + \sum_{j \in N^{cut}} N_j(x) [H(x) - H(x_j)] a_j^* \\
&+ \sum_{k \in N^{tip}} N_k(x) \sum_{\alpha=1}^{12} [F_\alpha(x) - F_\alpha(x_k)] b_{k\alpha}^* \\
&+ \sum_{I \in N^{interface}} N_I(x) \Psi(x) c_I^*
\end{aligned} \tag{6}
$$

Normalized stress intensity factors and time are as follows:

$$
\begin{gathered}
K_I^* = \frac{K_I}{\sigma_0\sqrt{\pi a}}, \quad K_{II}^* = \frac{K_I}{\sigma_0\sqrt{\pi a}}, \quad K_{IV}^* = \frac{e_{33}}{h_{33}} \frac{K_{IV}}{\sigma_0\sqrt{\pi a}} \\
T = \frac{c_L t}{h}, \qquad c_L = \sqrt{\frac{C_{33}}{\rho}}
\end{gathered} \tag{7}
$$

3. Model and method

The calculation model is shown in Figure 1. Here. H=40mm,2a=4.8mm. Mater.1 is PTZ-5H, Mater.2 is PTZ-6B. The plate is poled along y-direction. The mechanical load and electric displacement load act on the upper and lower surfaces. Where, $\sigma_{yy} = \sigma(t) = \sigma_0 H(t), D_y = \lambda h_{33} / e_{33}\sigma(t)$.

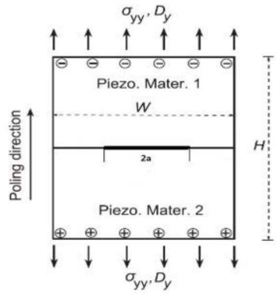

Figure 1. Model geometry and its notations for an interface crack in piezoelectric bimaterials.

4. Numerical evaluation results

The extended finite element mesh for interface crack is shown in Figure 2. It is easy to see that the crack cuts through mesh elements and there are not a lot of elements around the crack.

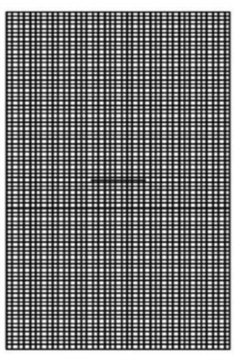

Figure 2. Meshing of interface crack.

Figure 3 and Figure 4 further present the stress and electric displacement fields for a horizontal subinterface crack in PZT-5H/PZT-6B subject to the electromechanical loading. The influence and the difference of bimaterials are clearly seen from these plots for subinterface crack problems.

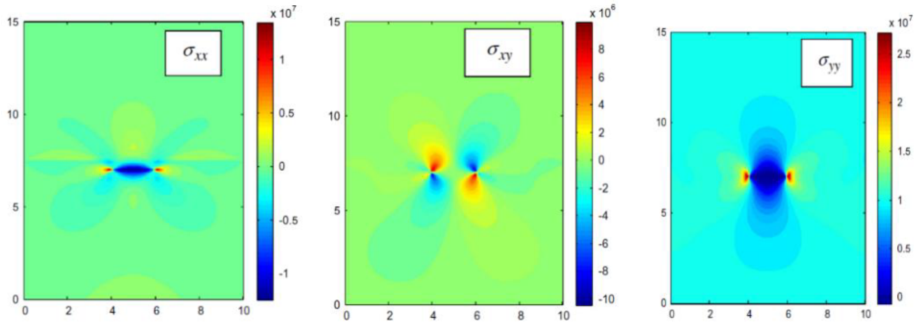

Figure 3. Normalized stress plots.

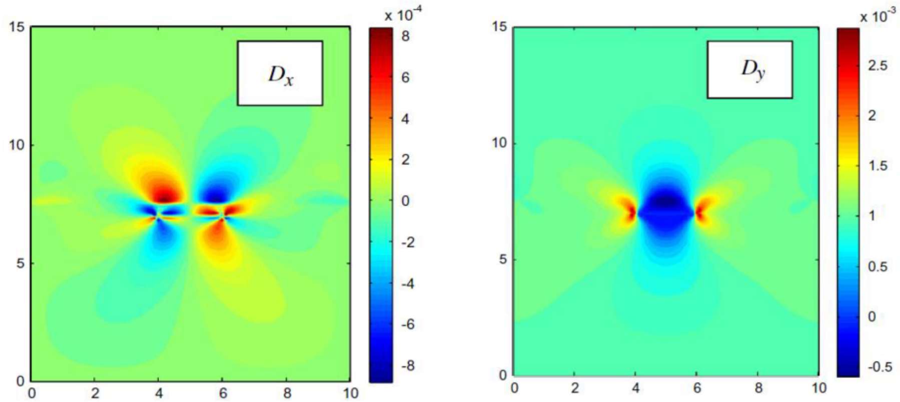

Figure 4. Normalized electric displacement.

In Figure 5, IFs are calculated for different inclination angles of the crack using XFEM. The normalized results of IFs obtained using XFEM closely follow the results of BEM.

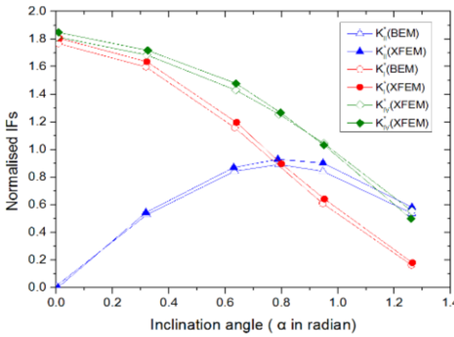

Figure 5. Variations of normalized IFs versus α.

Figure 6 depicts the variation of normalized IFs (K_I*, K_{II}* and K_{IV}*) with respect to inclination angle α, for the five cases of electromechanical loadings(λ=0,1,2,3,4). The results show that normalized IFs K_I* and K_{II}* are almost independent of the electrical loadings. Whereas the normalized electric displacement intensity factor K_{IV}* depends upon the electrical loading and it increases with an increase in electric displacement loadings. It may also be noted that IFs converge for larger value of inclination angle.

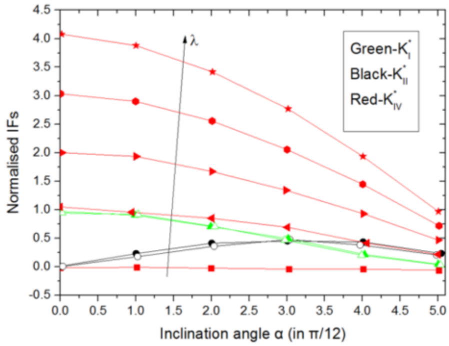

Figure 6. Variations of normalized IFs versus α (for different electromechanical loadings).

Figure 7 shows that normalized IFs K_I*, K_{II}* and K_{IV}* increase with respect to increase in crack length. It is seen that the difference in normalized IFs with respect to crack length also depend upon the inclination angle. In case of normalized K_I*, this difference decreases with respect to the increase in inclination angle. But the difference increases with increase in inclination angle in case of normalized K_{II}*. The variation of normalized K_{IV}* with respect to crack length is same as in case of normalized K_I*.

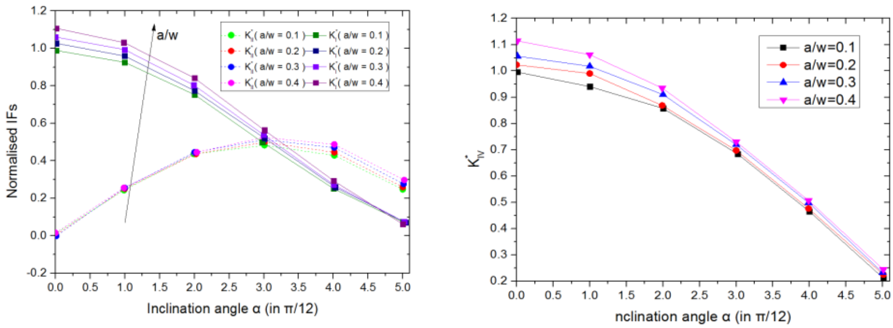

Figure 7. Normalized IFs (K_I*, K_{II}*and K_{IV}*) respect to α for different crack lengths.

It concludes that:

- The results of XEFM are found in good agreement with BEM solutions.
- The peak values of dynamic stress intensity factor decreases as the electrical load increases. It means that the positive electric field assists the occurring of fracture, while the negative electric field retards the fracture.
- The value of dynamic stress intensity factor is not equal to zero when t=0. It relates to the strength of electric shock. While, the elastic wave caused by mechanical force shock need some time to influence crack.

5. Conclusions

We have successfully applied the XFEM and the level set method to solution interface crack with impact loading problems. It is shown that the XFEM exhibits an excellent performance and more convenience compared to other existing methods in dealing with crack. The XEFM has the following advantages: the computational grid is independent of the crack; do not need to set the singular element; have higher accuracy and good results can be obtained with less and coarser elements.

Acknowledgements

We thank the Ningxia Natural Science Foundation for their support. (2022AAC03339)

References

[1] Y. E. Pak. Linear electro-elastic fracture mechanics of piezoelectric materials[J]. Fract 54(1):79–100(1992), doi: 10.1007/BF00040857.
[2] Y. E. Pak. Crack extenion force in a piezoelectric material[J]. Appl Mech 57(3):647–653(1990), doi: 10.1115/1.2897071.
[3] H. Sosa. Plane problems in piezoelectric media with defects[J]. Solids Struct 28(4):491–505(1991), doi: 10.1016/0020-7683(91)90061-J.
[4] T. Y, Zhang, J. E. Hack. Mode-III cracks in piezoelectric materials[J]. Appl. Phys 71(12):5865-5870(1992), doi: 10.1063/1.350483.
[5] B. L. Wang, J. C. Han, and S. Y. Du. Electroelastic fracture dynamics for multilayered piezoelectric materials under dynamic anti-plane shearing[J]. Solids Struct 37(38):5219–5231(2000), doi: 10.1016/S0020-7683(99)00218-8.
[6] Pang Y, Wang YS, Liu JX, Fang DN.: A study of the band structures of elastic wave propagating in piezoelectric/piezomagn/piezomagnetic layered periodic structures[J]. Smart Materials and Structures 19(5):055012(2010), doi: 10.1088/0964-1726/19/5/055012.
[7] CZ Zhang. A 2D hypersingular time-domain traction BEM for transient elastodynamic crack analysis[J]. 35(1):17-40(2002), doi: 10.1016/S0165-2125(01)00081-6.
[8] Ang. WT, Athanasius L. Dynamic interaction of multiple arbitrarily oriented planar cracks in a piezoelectric space: A semi-analytic solution[J]. European journal of mechanics A-solids 30(4):608-618(2011), doi: 10.1016/j.euromechsol.2011.03.003.
[9] Matin. MA, Akai. D, Ozaki. K, Kawazu. N, Hanebuchi. M, Sawada. K, Ishida. M. Dynamic behavior of a new surface-micromachined piezoelectric material actuated micro-mirror device[J]. COMPUTATIONAL MATERIALS SCIENCE, 50(8):2311-2318(2011), doi: 10.1016/j.commatsci.2011.02.041.
[10] Bechet E, Scherzer M, Kuna M. Application of the X- FEM to the fracture of piezoelectric materials[J] International Journal for Numerical Methods in Engineering, 77(11):1535-1565(2009), doi: 10.1002/nme.2455.
[11] Rybicki E. F, Kanninen M. F.: A finite element calculation of stress intensity factors by a modified crack closure integral[J]. Engineeing Fracture Mechanics, 9(4):931-938(1977), doi: 10.1016/0013-7944(77)90013-3.